The influence of aspect ratios in the physical aspects of the wake behind a blunt-trailing-edged body

Eduardo Silveira Molina, molina@ita.br
Marcos Aurélio Ortega, ortega@ita.br
Roberto da Motta Girardi, girardi@ita.br
ITA - Technological Institute of Aeronautics, São José dos Campos, SP, 12228-900, Brasil

Abstract.*This work focuses on the influence of the boundary thickness upon the physical parameters (Strouhal number and base pressure coefficient, for example) of the near wake of a blunt-trailing-edge body when the aspect ratio was varied. In contrast to the circular cylinder case, the present model has a boundary layer separation point defined and fixed. This permits a better assessment of the vital influence of the boundary layers upon the wake, in a net and clear way. Data are obtained experimentally by means of a Laser Doppler Anemometer (LDA) which is a especial tool to perform measurements in low Reynolds number. Experiments were undertaken in the range of Reynolds number between 600 and 3000. In the present study, the results show that the boundary layer thickness is inversely proportional to the Strouhal number and the mean circulation.*

Keywords: *bluff body, near wake, LDA*

1. Introduction

In studies of the turbulent wake of a bluff body, several authors, for example Roshko (1954) and Bearman (1967), have attempted to establish similarities of fluid flow properties between bodies of different shapes. The authors also introduced their own universal Strouhal numbers which were found to remain constant for several different two-dimensional bluff bodies. Simmons (1977) studied the similarities between two-dimensional bodies with different boundary layer separation angles. The author found that the formation length have similar relations with the boundary layer separation angle.

Relative to this special geometry studied here, Bearman (1965), the first one to perform hot-wire measurements with this type of body with aspect ratio, c/h, equal to 6 and Reynolds number of $1.4\text{x}10^5$, investigated the flow field with the advent of splitter plates in order to asses the possibility of drag reduction and how those factors would influence the formation length. The base pressure coefficient was approximately -0.58 and the Strouhal number was 0.24. Following the attempt of drag reduction of Bearman (1965), Park $et\ al.$ (2006) investigated a new passive device, the basic idea was to install small tabs at the upper and lower trailing edges of the body ($AR = 6.33$) with the aim of mismatching the vortex shedding process and a consequent vortex strength and overall drag reduction, the study involved both experimental ($Re = 20000 - 80000$) and numerical treatments ($Re = 420$ and 4200). Ryan, Thompson and Hourigan (2005) studied the three-dimensional transition in the wake using essentially a numerical tool in order to perform a Floquet analysis of the near wake flow for $AR = 2.5$, 7.5 and 17.5.

This investigation was carried out in order to examine more fully the influence of the boundary layer thickness of a two-dimensional blunt-trailing-edge body varying the aspect ratio and the Reynolds number upon the physical parameters of the respective near wake.

2. Models Descriptions

One wishes to investigate experimentally the two-dimensional flow of an incompressible fluid about the bluff body as depicted in Fig. 1a. The body consists of a fix aerodynamic elliptic nose

section followed by a parallel-sided section. The aspect ratio, AR, is defined by c/h where c is the chord and h is the body base height, Fig. 1a. Due to the small length working section, the values of the aspect ratios chosen are: $AR = 3$, $AR = 5$ and $AR = 7$. The front part of the elliptic nose section was fixed relative to the $AR = 3$ configuration, with semi-major and semi-minor axes of $5h/2$ and $h/2$, respectively, followed by a parallel-sided section of length $h/2$. For the other two bodies, the same elliptical nose was maintained, while the length of the afterbody was varied according to the desired aspect ratio. The reason for keeping those overall proportions is because the resulting flow is quite smooth down to the separating points, without running the risk of a separation, or an eventual perturbation at the front shoulders (the points where the front elliptical arc touches the upper and lower flat plates) (Bearman, 1965). The present body was studied extensively by the Prof. P.W. Bearman in the 60's (Bearman 1965, 1967) for this reason we shall call the body of Bearman.

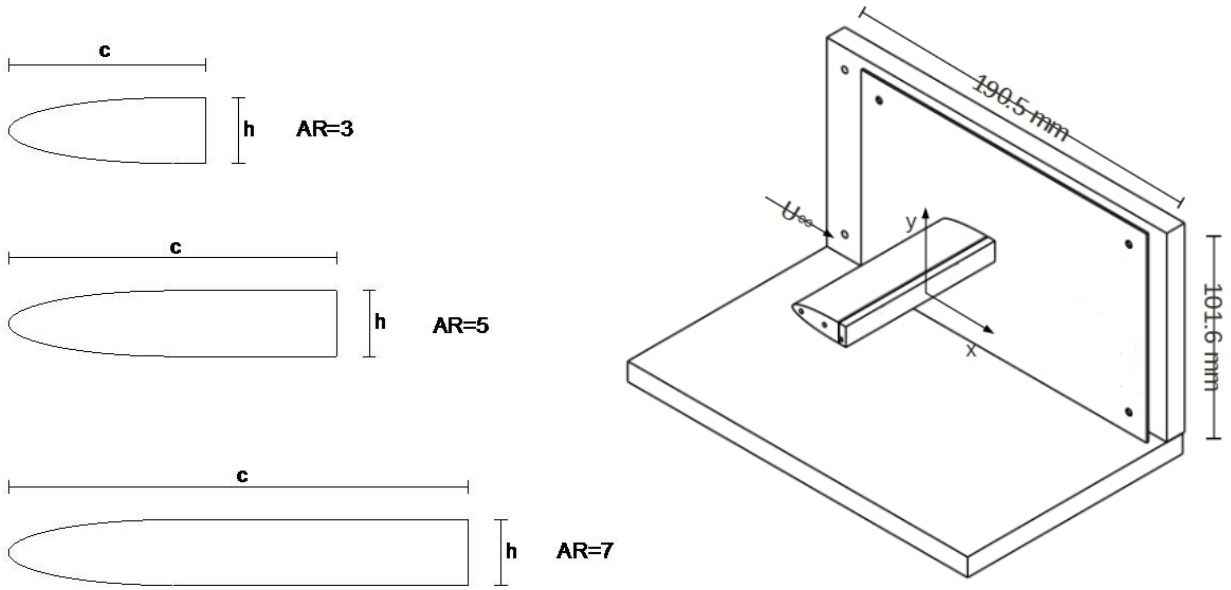

(a) (b)

Figure 1: (a) Cross-section view of the model; (b)Isometric view of the working section with the end-plates and the model.

3. Experimental Apparatus

All measurements were carried out in the open-circuit low-speed wind tunnel TSI 8390 at the Laboratory Prof. Feng in the Aeronautical Institute of Technology (ITA). The working section is $190.5\ mm$ long and has a square cross-section of $101.6\ mm$. The body base height (h) is $10\ mm$. The velocity was varied from $1m/s$ to $5m/s$. Finally, the blockage ratio is 9.8%.

A commercial Dantec fibre-optic LDA-system arranged in a backscatter mode was employed with a focal length of $800\ mm$. For measurements of the streamwise (U) and cross-wise (V) velocity components, respectively, the green (wavelength $514.5nm$) and the blue ($488nm$) coherent lights of an argon-ion laser was used. The signals of the photomultipliers were analyzed using the BSAFlow Software (Dantec Dynamics, 2005). The ellipsoidal measurements volumes were each approximately $0.10\ mm$ in width and $0.13\ mm$ in length. The number of samples collected at each position was typically 50000 and a transit time weighting was applied to the data. The computer-controlled 2D-traverse system had a positional accuracy of about $0.1mm$. The uncertainty in U was estimated in ± 0.005.

At previous running from $4m/s$ to $22m/s$, the boundary-layer thickness at the mid-station of the

working section was measured and the result was approximately $6mm$ (Araujo, 2008). Thus, end-plates were attached at $10mm$ from either wall to reduce the inflow from the wind tunnel boundary layer to the low pressure region behind the model. The end plates were designed following recommendations by Stansby (1974), as one can see in Fig. 1b. They were rectangular shaped plates $10.1h$ height, $16.0h$ long and the distance between body axis and the leading edge of end-plate was $7.0h$. The model is attached to the end-plate. One of the end-plates was made of acrylic so the laser beam can intersect with each other inside the working section. Both the other end-plate and the parallel-sided section were made of aluminium painted in black to avoid laser beam reflections and the elliptic nose was made of wood.

The origin of the coordinate system was placed at the body axis (midspan position) as shown in Fig. 1b. The streamwise and cross-wise directions are denoted x and y, respectively. The free stream velocity (U_∞) was determined from repeated measurements using LDA at $x = -7h$ and $y = 2.5h$. When scaled with U_∞ the crosswise velocity at this position was within ± 0.006.

In previous low-velocities measurements, $U_\infty \approx 1m/s$, the seeding particles were responsible for generating a high turbulence level ($Tu = U_{rms}/U_\infty$) in the beginning of the working section. So it was decided to develop a flow rectifier with $0.4m$ x $0.4m$ x $1.0m$, see Fig. 2, in order to decrease this high turbulence level and produce a more uniform flow. The seeding was provided by a oil-fog generator nozzle type connected to the lower part of the flow rectifier which is attached at the entrance of the wind tunnel. Inside this rectifier were placed honeycombs and screens. The suction air is regulated by a sliding window in the front part. In the upper part, there is a tube with a valve connected to the exhaust fan to remove the excess of the particles avoiding their exit to the ambiance, consequently, contaminating the air and damaging the equipment.

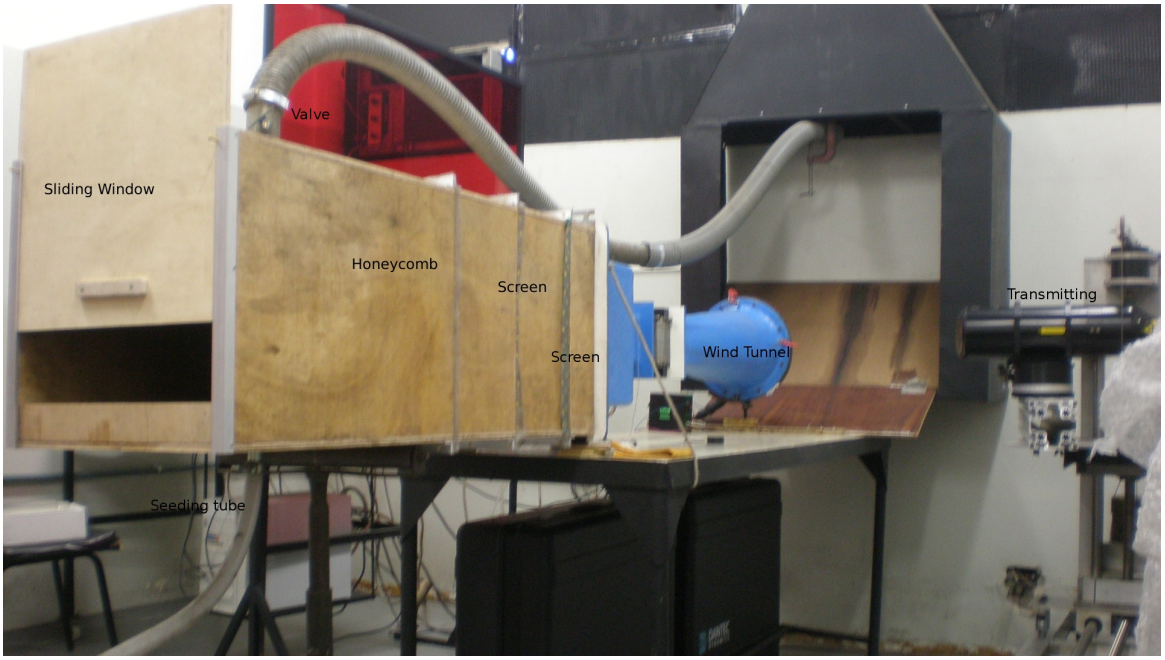

Figure 2: Flow rectifier.

The Figure 3 shows the results of the turbulence level at the beginning of the working section with and without the flow rectifier. As one can appreciate for low velocities, the turbulence level decreased greatly. It is well known that the seeding particles increase the turbulence level of the wind tunnel (Kähler, Sammler and Kompennahns, 2002). From previous measurements (Araujo, 2008), the turbulence level without the seeding particles was approximately 0.25% measured with a hot-wire anemometer from free-stream velocities varying from $1m/s$ to $15m/s$.

The measurement of the tip boundary layer profiles was made at a point upstream of the trailing

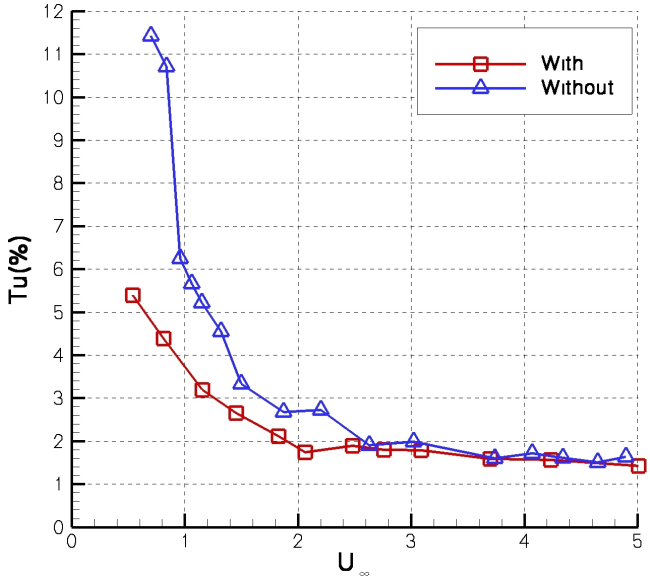

Figure 3: Turbulence level as function of the free-stream velocity, with and without the flow rectifier.

edge ($x = -0.1mm$), relative to the centre-span plane of the model, to avoid the recirculating flow downstream of the blunt base. The physical boundary layer thickness was defined as the distance perpendicular of the model surface where the maximum velocity was reached (U_s, separation point velocity). The vortex shedding frequency was measured by placing the laser beams in the wake of the model. The location of the laser beams was approximately $x/h = 1.5$ and $y/h = 1.5$, but this position was slightly different for each test case to get the best periodic signals.

4. Results

The boundary layers profiles for $AR = 3$, $AR = 5$ and $AR = 7$ are displayed in Figs. 4 and 5 with the Blasius theoretical laminar solution for the flat plate. The first aspect to stress is that the boundary layers at the tips of the body base, just before the separation point are always laminar and the profiles showed a good agreement with the theoretical solution, except for $AR = 7$ and $Re = 3000$ where we believe that the boundary layer presents a transitional kind of state, the Fig. 5 supports this assertion.

The Figure 6a shows the profiles of the streamwise root-mean-square velocities (u_{rms}) dimensionless by the free-stream root-mean-square velocity (U_{rms}) along the boundary layer for $AR = 7$, $Re = 600$ and $Re = 3000$. From this plot, we can perceived that possibly exists a generation of turbulence inside the boundary layer due to a higher turbulence level when compared with the free-stream. Thus, to confirm this statement, the spectral density (energy spectrum) is plotted in Fig. 6b at the same position ($y/h = 0.06$) inside the boundary layer for both Reynolds number and outside the boundary layer ($y/h = 0.3$) for $AR = 7$ and $Re = 3000$. As one can see for low frequencies, there is a generation of high energy when compared with the almost discrete spectrum of $Re = 600$. The distinct energy peak that appears in all cases indicates the vortex shedding frequency. However, the shedding amplitude is higher inside the boundary layer ($y/h = 0.06$) on the order of $5\text{x}10^{-3}m^2/s$ when compared with the amplitude outside the boundary layer ($y/h = 0.30$), $1\text{x}10^{-3}m^2/s$.

Based on the profiles presented previously, the tip boundary layer displacement and momentum thickness and the shape factor were calculated and they are defined in Eq. 1, 2 and 3, respectively:

$$\delta^* = \int_0^\delta \left(1 - \frac{u}{U_s}\right) dy \tag{1}$$

$$\theta = \int_0^\delta \frac{u}{U_S}\left(1 - \frac{u}{U_s}\right) dy \tag{2}$$

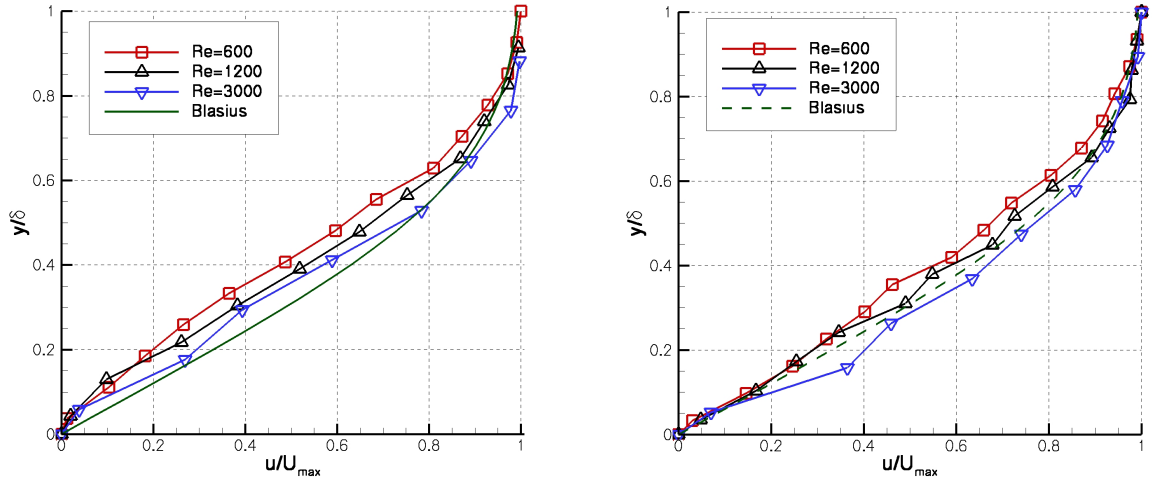

(a) (b)

Figure 4: Comparison of boundary layer profiles for different Reynolds number. (a) AR=3; (b) AR=5.

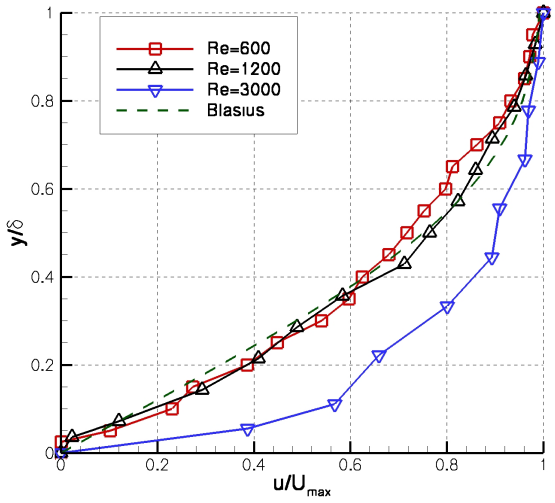

Figure 5: Comparison of boundary layer profiles for different Reynolds number. AR=7.

$$H = \frac{\delta^*}{\theta} \tag{3}$$

These values are shown on Fig. 7 as function of Re^* , dimensionless by $h^* = h + 2\delta^*$. As one can observed, for a fixed aspect ratio the boundary layer thickness (displacement and momentum) diminished with the growing of the Reynolds Number. On the other hand, for a fixed Reynolds number the boundary layer thickness grows with the growing of the aspect ratio, especially in $Re \approx 600$ where the viscosity plays a more important role when compared to higher Reynolds number. It is important to point out the unexpected behaviour of the boundary layers thickness for $AR = 7$. The Figure 8a shows the shape factor H as function of both Reynolds Number and aspect ratio. According to Schlichting (2000), for the flat plate boundary layer the shape factor is 2.59 in the laminar region decreases to $H \approx 1.4$ in the turbulent region.

Searching a correlation of the tip boundary layer with the traditional Strouhal number ($St = f\ h/U_\infty$), we decided to measured the shedding frequency of the three aspect ratios for a wide

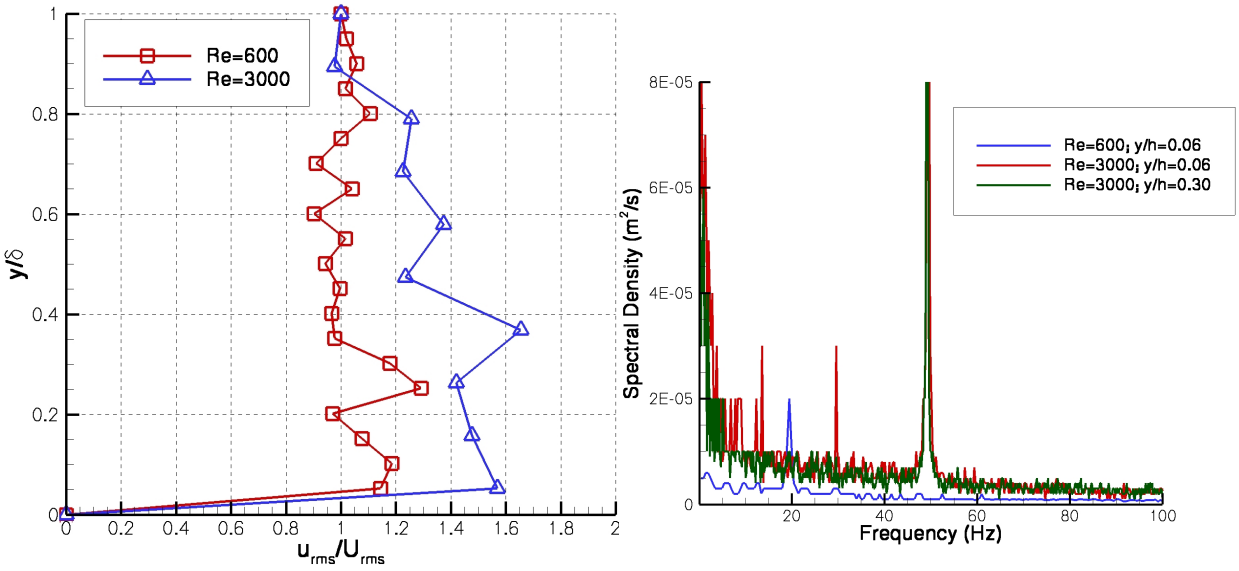

(a) (b)

Figure 6: (a) Streamwise root mean square velocity along the boundary layer for AR=7. (b) Spectral density (Energy spectrum) at y/h=0.06. $AR = 7$, $Re = 600$ and $Re = 3000$

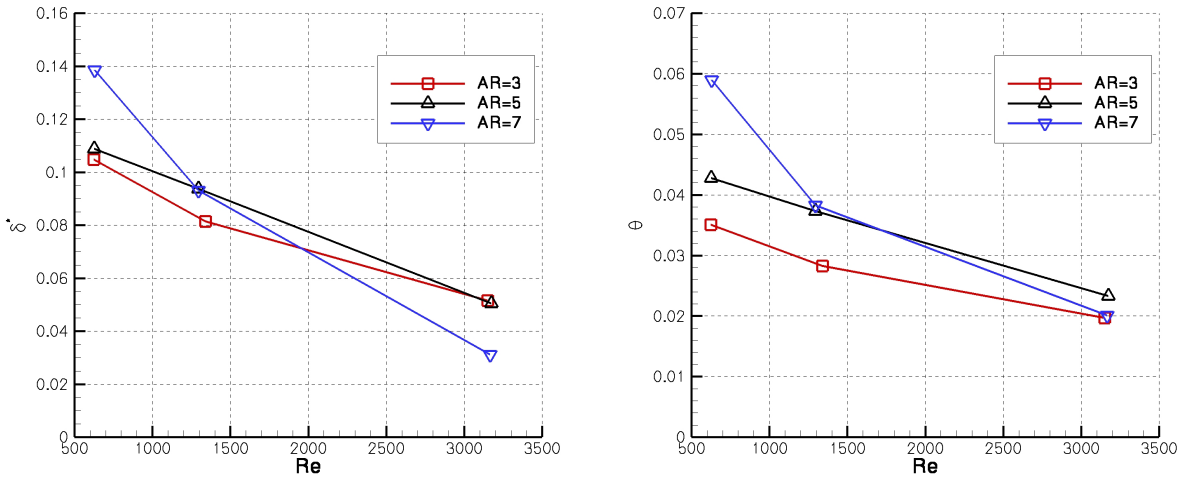

(a) (b)

Figure 7: Tip boundary layer's thickness as function of the Reynolds number dimensionless in reference to the body base height. (a) Displacement thickness; (b) Momentum thickness.

Reynolds number range $(600-3000)$, since we did not found this information in the literature. The dimensionless frequencies are displayed in Fig. 8b as function of the Reynolds Number. Independently of the aspect ratio, the tendency of the curves $StxRe$ is basically the same: the shedding frequency grows with the growing of the Reynolds Number as occurs with the circular cylinder for low Reynolds number (Williamson, 1996). Moreover, the frequency augments with diminishing of the aspect ratio for a fixed Re.

As can be seen from Figs. 8b and 7 , the behaviour of the shedding frequency has a straight connection with the boundary layer's thickness. For a fixed Reynolds number the boundary layer thickness increased while the Strouhal number decreased with the increased of the aspect ratio. This possibly occurs due to a thicker boundary layer difficult the rolling of the free shear layer to form

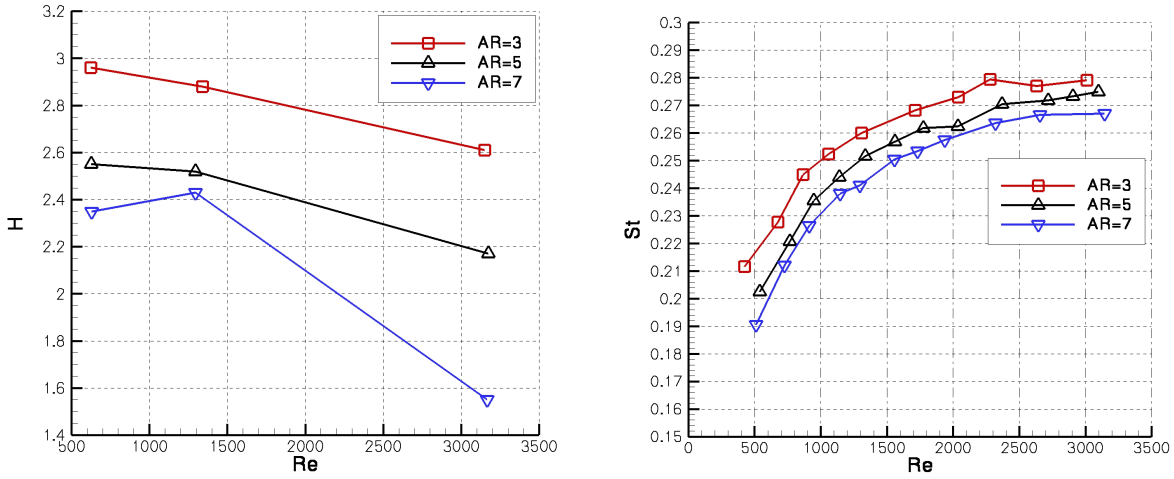

(a) (b)

Figure 8: (a) Shape factor as function of Reynolds number; (b) Shedding frequency as function of the Reynolds Number.

a new vortex, increasing the period of the vortex formation consequently, decreasing the shedding frequency and probably increasing the vortex formation length. On the other hand, for a fixed aspect ratio, the tip boundary layer decreased with the growing of the Reynolds number in contrast to the increase of the vortex shedding frequency. The two conditions seems to be consistent.

The variation of the boundary layer thickness with the Reynolds number shows that these parameters are not the only ones that affect the Strouhal number. There is something else that is driving the vortex shedding frequency. The results for $AR = 7$ can confirm this statement because for the largest Reynolds number studied ($Re = 3000$), the boundary layer thickness is smaller than in the others aspect ratios.

A summary of critical values are compiled in Tab. 1, where are presented two others Strouhal numbers , St^* and St_s^*, besides the traditional one. St^* and St_s^* are both dimensionless by $h^* = (h + 2\delta^*)$. Furthermore, St_s^* is also dimensionless by U_s as opposed to St^* which is dimensionless by U_∞. It can be seen by Tab. 1 that St^* and St_s^* were found to form an approximate constant relationship with the Reynolds number especially, for $Re = 1200$ and $Re = 3000$. According to Fage and Johansen (1928), the base pressure coefficient is directly related to the velocity on the separation point and this relationship is given by:

$$C_{pb} = 1 - \left(\frac{U_s}{U_\infty}\right)^2 \tag{4}$$

$$C_{pb} = 1 - K^2 \tag{5}$$

where U_∞ is the free stream velocity, U_S is the separation point velocity (velocity at the border of the boundary layer) and K is the ratio between both.

An important aspect to call attention is how different is the behaviour of the distributions of C_{pb} for $AR = 7$, the highest value of the aspect ratio measured here, when confronted to the other ones, as one can see in Fig. 9. The base pressure becomes more negative with the increase of the Reynolds Number, but for the other AR's we have exactly the contrary. It is important to point out that for $Re = 1200$ and $Re = 3000$, the values of the base pressure coefficient are apparently closed with each other with a kind of asymptotic behaviour as the Reynolds Number grows. With this notable

Table 1: Summary of the results for the aspect ratios studied.

Re	St	St^*	St_s^*	K	C_{pb}	$\Gamma/U_\infty h$	$\Gamma/U_\infty h^*$
AR=3							
600	0.222	0.269	0.200	1.347	-0.816	4.080	3.373
1200	0.259	0.302	0.236	1.277	-0.631	3.146	2.705
3000	0.279	0.301	0.251	1.225	-0.500	2.690	2.493
AR=5							
600	0.206	0.251	0.198	1.269	-0.611	3.903	3.202
1200	0.249	0.296	0.241	1.228	-0.509	3.030	2.551
3000	0.274	0.302	0.249	1.210	-0.465	2.674	2.429
AR=7							
600	0.196	0.247	0.218	1.128	-0.273	3.251	2.582
1200	0.241	0.286	0.238	1.199	-0.438	2.983	2.515
3000	0.267	0.284	0.235	1.206	-0.454	2.722	2.563

features, we believe that for low values of the aspect ratios the base pressure is very sensitive to the growing of the Reynolds Number because the flow is more influenced by the streamlined elliptical nose. As the aspect ratio grows ($AR = 7$), the flow along the body walls just before the separation tends a similar pattern even for a rather variation of the Reynolds number.

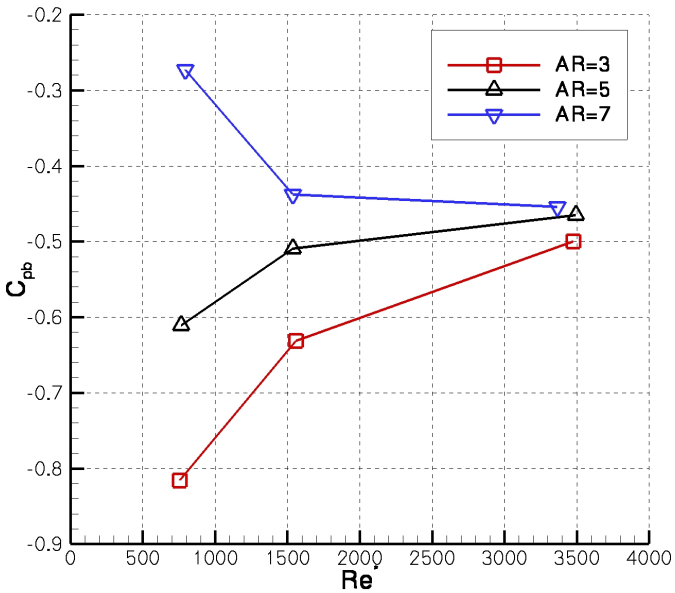

Figure 9: Base pressure coefficient as function of the Reynolds Number.

Following the previous dimensionless, the mean circulation that leaves the body during the release of a single vortex is dimensionless using both Strouhal numbers , St and St^*, and the rate K in accordance with Eq. (6).

$$\frac{\Gamma}{U_\infty h} = \frac{K^2}{2St} \tag{6}$$

It is worth to remember that this mean circulation is not necessarily the one encountered downstream in a single vortex, what is a consequence of a certain amount of difusion due mainly to interactions between the growing vortices at the formation region. However, some notable features were found in this parameter. There is a higher decrease in the mean circulation as the Reynolds grows for $AR = 3$ and 5 when compared to $AR = 7$ as as a consequence of the decrease of K for $AR = 3$ and 5. A probably explanation for this fact is if the Reynolds number is low, the flow behind the body can influence more deeply the velocity at the separation point (U_s). Another possibly explanation, for $Re = 600$ the effective angle at the separation point ($d\delta^*/dx$) diminish with the growing of the aspect ratio leading to a lower value of K, consequently, a lower centrifugal force imposed by the pressure gradient leading to an increase in the base pressure coefficient and in the mean circulation value. In respect of the mean circulation, it was found that when dimensionless by h^*, it remains approximately constant as the Reynolds number grows supporting one more time the assertion of the similar pattern of $AR = 7$.

5. Conclusion and comments

It is interesting to note that in a boundary layer study, several parameters can be analyzed for a better understanding of the flow around a blunt body principally due to the fixed point of separation, the main feature of this body, which facilitates this type of study. The main goal here is to asses the vital influence of the aspect ratio changing the boundary layer thickness in the global parameters, making correlations between then, for example Strouhal number, base pressure coefficient and boundary layer thickness. As the aspect ratio grows the flow around the model behaves more like a flat plate losing the influence of the aerodynamic elliptic nose. All the boundary layers profiles performed here were compared with the Blasius laminar solution for the flat plate, in a consequence, they found to agree with the theoretical solution, except for $AR = 7$ and $Re = 3000$. This subject will be better investigated, however, the instability of the free shear layer can be the responsible for this premature transition. When a correlation of the tip boundary layer with the traditional Strouhal number were made, the tip boundary layer decreases consequently, the Strouhal number increases as the Reynolds number grows, we realize that there is something else driving the shedding frequency due to the different behaviour of $AR = 7$ model especially at $Re = 3000$, however the St^* remains constant. At the present moment, Direct Numerical Simulations are being made to try to explain and complement the present analysis of the experimental results that remain open.

6. ACKNOWLEDGEMENTS

The authors would like to acknowledge the financial support provided by CNPq, the Brazilian National Council of Research and Development, through grant 303184/2007-8, and Fapesp, the State of São Paulo Foundation for the Support of Scientific Research, through grant SP/2549/2007.

7. REFERENCES

Araújo, T.B., "Influência do ângulo de separação na esteira próxima de escoamentos bidimensionais sobre corpos rombudos.", Dissertação (Mestrado em Aerodinâmica, Propulsão e Energia) - Instituto Tecnológico de Aeronáutica, São José dos Campos, 2008.

Bearman, P.W., “Investigation of the flow behind a two-dimensional model with a blunt trailing edge and fitted with splitter plates". J. Fluid Mech., 21:241-255, 1965.

Bearman, P.W., “On vortex street wakes". J. Fluid Mech., 28:625-641, 1967.

Dantec Dynamics. "BSA Flow Software. Version 4 Installation and UserâĂŹs Guide.", 2005.

Fage, A. and Johansen, F.C., "The structure of vortex sheets." Proc. Roy. Soc. Lond. A, 1928.

Kähler C, Sammler B, Kompenhans J. Generation and control of tracer particles for optical flow

investigations in air. Experiments in Fluids, 33:736-742, 2002.

Park, H., Lee, D., Jeon, W., Hahn, S., Kim, J., Kim, J., Choi, J., Choi, H., "Drag reduction in flow over a two-dimensional bluff body with a blunt trailing edge using a new passive device.". J. Fluid Mech., 563:389-414, 2006.

Roshko, A., "On the development of turbulent wakes from vortex streets". NACA Report, 1954.

Ryan, K., Thompson, M.C. and Hourigan, K., "Three-dimensional transition in the wake of bluff elongated cylinders". J. Fluid Mech., 538:1-29, 2005.

Schlichting, H., "Boundary-layer theory.", Springer, 2000.

Simmons, J.E.L. Similarities between two-dimensional and axisymmetric vortex wake. Aero. Quarterly 26:15-20, 1977.

Stansby, P.K., "The effect of end plates on the base pressure coefficient of a circular cylinder". R. Aeronaut. J., 78:36-37, 1974.

Williamson, C.H.K., "Vortex dynamics in the cylinder wake." Annu. Rev. Fluid Mech., 28:477-539, 1996.

8. Responsibility notice

The author(s) is (are) the only responsible for the printed material included in this paper